Investigation of field-effect passivation and interface state parameters at the Al_2O_3/Si interface

Wensheng Liang, Klaus J. Weber, Dongchul Suh, Yongling Ren

Centre for Sustainable Energy Systems, College of Engineering and Computer Science, The Australian National University, Canberra, ACT 0200, Australia

Abstract: The field-effect passivation of Al_2O_3 films deposited by plasma–assisted atomic layer deposition (PA-ALD) for p- and n-type c-Si was investigated. The effective surface recombination velocity (S_{eff}) at the PA-ALD Al_2O_3/Si interface was obtained by both positive corona charge and lifetime measurements with a gate bias voltage on a metal-oxide-silicon-oxide-metal (MOSOM) structure. The phenomenon of little drop of S_{eff} with high positive voltage applied on p-type wafer passivated by PA-ALD Al_2O_3 was observed which is consistent with the slight S_{eff} decrease with long time positive corona charge. Energy dependent capture cross sections for electrons and holes were calculated simulated for the PA-ALD Al_2O_3/c-Si interface by a method proposed by K. Yasutake. It was found that the maximum capture cross section of electrons is approximately 100 times larger than that of holes. Electron traps exist in PA-ALD Al2O3 layer which is illustrated by observed electron injection phenomenon for both positive and negative biased MOS structure. The ability of electron injection from silicon to Al2O3 can be controlled by changing Al2O3 deposition parameters.

Key words: atomic layer deposition, field effect passivation, solar cell, capture cross section, Al_2O_3

INTRODUCTION

Surface passivation of crystalline silicon(c-Si) currently is becoming increasingly important for high-efficiency and low-cost solar cells. The importance of surface passivation becomes greater as the substrate thickness for solar cells is reduced for the sake of material cost reductions. Currently three thin film materials are industrially employed for surface passivation of c-Si solar cells: thermally grown silicon dioxide(thermal SiO_2),[1] PECVD silicon nitride(a-SiNx:H) [2, 3] and amorphous silicon(a-Si :H)[4, 5]. But none of them is suitable to passivate boron doped emitter of n-type solar cells, which are relative insensitive to various impurities and defects compared with p-type material[6-8].

Thin films of Al_2O_3 on p- and n-type c-Si yield exceptionally low surface recombination velocities[9], enabling improved c-Si solar cell efficiencies[10]. PA-ALD Al_2O_3 limits the emitter saturation current density of B-diffused p+-emitters to 10 and 30 fA/cm^2 on 100 and 54 Ω/□ sheet resistance p+-emitters, respectively[11].The excellent passivation performance by PA-ALD Al_2O_3 layers is attributed to the high negative fixed charge density, about 1×10^{13}cm^{-2} after anneal, which is especially of benefit for boron doped emitters.

In this paper, the field-effect passivation of PA-ALD Al2O3 films was investigated by positive corona charge and lifetime measurements with gate bias voltage on a MOSOM structure. A phenomenon of slight passivation performance recovery upon long time positive corona charge was observed, which is confirmed by another experiment applying gradually increasing positive voltage on a similar wafer. The energy dependent capture cross section of holes and electrons for ALD Al2O3/c-Si interface was simulated according to a method proposed by K. Yasutake[12]. Electronic and chemical properties of ALD Al_2O_3/c-Si interface was given by capacitance-voltage(CV) measurements with fixed negative charge dendity $Q_f = 4.3\times10^{12}$cm^{-2} and interface state density $D_{it,midgap} = 7\times10^{10}$eV^{-1}cm^{-2}. Field effect passivation related with fixed negative charge density can be improved by increased Al2O3 surface potential, such as positive voltage bias or corona charge.

EXPERIMENT

Samples for lifetime measurement, corona charge and voltage-lifetime measurements were FZ p-type, 0.8 Ω-cm (100) wafers; some FZ n-type, 4 Ω-cm (100) wafers were used as well. C-V measurements were conducted on Cz p-type, 1-10 Ω-cm (100) and Cz n-type, 1-10 Ω-cm (100) silicon wafers. After a standard RCA clean, about 20nm Al2O3 layer was deposited in a Beneq TFS-200 ALD system at deposition temperature of 175°C with TMA and plasma oxygen as precursors. Passivation was activated by a 30min FGA anneal at 400°C. On some samples, ~5-8nm thick Al layers were grown to form a MOSOM structure for lifetime-voltage measurement[13]. Prior to C-V measurement, all insulator layers were removed from the rear of the samples, and Al dots with thickness of ~80nm were evaporated on the front and In/Ga contacts were formed on the rear of samples. Corona charging was carried out with a conventional setup[14] by applying voltage of +/−6 kV to a steel needle about 10 cm above the samples. Lifetime was measured on WTC-120 system at excess carrier concentration $\Delta n=1\times10^{15}$cm^{-3}.

RESULTS AND DISCUSSION

1. Surface recombination velocity (S_{eff}) with positive corona charge

The effective surface recombination velocity(SRV) S_{eff} is determined from the measured lifetime τ_{eff} using the equation[15]:

$$S_{eff} = \frac{W}{2}\left[\left(\tau_{eff} - \frac{W^2}{\pi^2 D}\right) - \frac{1}{\tau_b}\right] \quad (1)$$

Where W is the wafer thickness, D is the minority carrier diffusion constant, and τ_b is the bulk lifetime, which accounts intrinsic radiative and Auger recombination.

Fig.1 shows that excellent surface passivation was obtained by plasma-assisted ALD Al_2O_3 after annealing, with S_{eff}<1cm/s for both low resistivity p- and n-type samples and lifetimes nearly equal to the intrinsic bulk lifetime calculated by Kerr's Auger model[16]. When sufficient positive corona charge was applied to the sample, S_{eff} increased sharply due to a reduction in field effect passivation, as the positive corona charge cancels out some of the negative charge of the Al_2O_3 layer. However, as the positive charge density is further increased, S_{eff} only recovers to half its maximum value from 160cm/s to 85cm/s for p-type wafer. In contrast, for the n-type sample, S_{eff} decreases to ~5cm/s. After an IPA dip, which is indicated by the solid symbols, passivation performance approaches the original level for both samples.

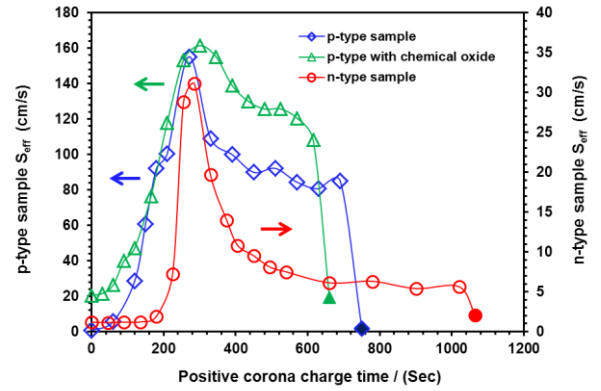

Fig.1. Measured S_{eff} values with a function of positive corona charging time. (Blue open squares: S_{eff} from FZ p-type 0.8Ω·cm wafer; Red open circles: S_{eff} from FZ n-type 4Ω·cm wafer; Green open triangles: S_{eff} from FZ p-type 0.8Ω·cm wafer with thin chemical SiOx synthesized during RCA clean; Solid end marks: S_{eff} obtained after samples were IPA dipped.

There are several possible reasons for this behavior. Firstly, the higher S_{eff} values with large positive corona charge density for all samples may be at least partly because the capture cross section of holes is larger than that of electrons, which will be studied in Part 2. With a large amount of positive charge on top of Al_2O_3 layer, SRH recombination at the interface of Al_2O_3/Si is limited by the hole concentration, therefore a larger capture cross section of holes than electrons implies a higher S_{eff} value. Secondly, the higher S_{eff} values could be the result of an inhomogeneous surface distribution of the negative fixed charges built into the Al_2O_3 film[14]. Finally, the difference in S_{eff} values between n and p type substrates could be the result of recombination in the depletion region [7].

In Fig.1, the presence of interfacial silicon oxide synthesized during RCA clean results in higher S_{eff}. This is not a result of decreased charge density since applying more negative corona charge doesn't change this result. Furthermore, the sample with chemical oxide between silicon and Al2O3 shows lower S_{eff} at inversion range, which indicates that chemical recombination parameters could be modified with the presence of chemical SiO2. Three samples in Fig.1 illustrate very similar fixed negative charge density, as the largest S_{eff} for three curves was found after similar positive corona charging time

2. Capture cross section calculation for interface of Si/PA-ALD Al_2O_3

The effective surface recombination velocity S_{eff} defined at the edge of the surface depletion region can be calculated by standard Shockley-Read-Hall (SRH) theory[17, 18]. For a continuum of noninteracting interface state, S_{eff} is obtained by the following integration over the band gap:

$$S_{eff} = \frac{V_{th}(n_s p_s - n_i^2)}{\Delta n}\int_{E_V}^{E_C} \frac{D_{it}(E)}{\frac{n_s + n_1(E)}{\sigma_p(E)} + \frac{p_s + p_1(E)}{\sigma_n(E)}} dE \quad (2)$$

where

$$n_1 = n_i \exp\left(\frac{E - E_i}{kT}\right), \quad p_1 = p_i \exp\left(\frac{E - E_i}{kT}\right) \quad (3)$$

n_i is the intrinsic carrier concentration, E the interface trap energy level, E_i the intrinsic Fermi level, E_c is the bottom of the conduction band, E_v is the top of valence band, V_{th} is the carrier thermal velocity, k is the Boltzman constant, T is the absolute tempreture, Δn is the injection carrier concentration, D_{it} is the interface state density, and σ_n, σ_p are the capture cross sections for electrons and holes, respectively.

The concentration of electrons and holes at the surface of silicon can be written as:

$$n_s = n_i e^{\beta(\varphi_s - \phi_n)}, \quad p_s = n_i e^{\beta(\phi_p - \varphi_s)} \quad (4)$$

Where $\beta = q/kT$, Φ_n and Φ_p are the quasi-Fermi potentials for electrons and holes, respectively, φ_s is the surface band bending.

By differentiating Eq.2 with respect to φ_s, the band bending $\varphi_{s,max}$ at which S_{eff} is at maximum can be obtained from $dS_{eff} / d\varphi_s = 0$, which gives

$$\varphi_{s,\max} = \left(\frac{kT}{2q}\right)\ln\left(\frac{\sigma_p(E)(p_0 + \Delta n)}{\sigma_n(E)(n_0 + \Delta n)}\right) \quad (5)$$

From Eq.5, the σ_p / σ_n can be estimated.

The D_{it} distribution and Q_f were determined from C-V measurements. The defect density was calculated using the Castagne method[19] and the result is shown in Fig.2. A high negative fixed charge Q_f = 4.3×10^{12}cm^{-2} was obtained. We note that the interface state density reported here, $D_{it,midgap}$ = 7×10^{10}eV^{-1}cm^{-2} , is smaller than published data elsewhere.

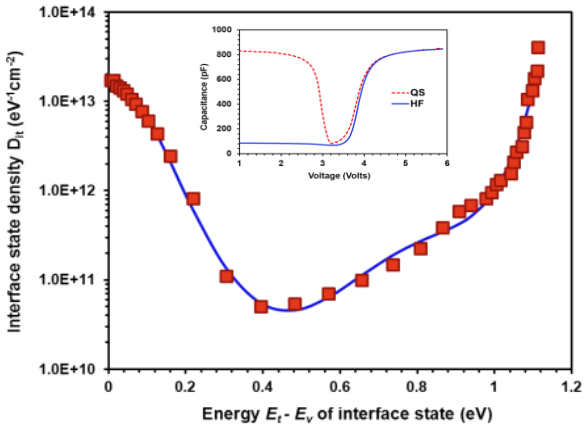

Fig.2 Capacitance voltage curves and interface state density as a function of the energy position E=E_t-E_v relative to the silicon valence band edge for a PA-ALD Al2O3 layer. The interface state density is $D_{it,midgap}$ = 7×10^{10}eV^{-1}cm^{-2}. The blue line marks the defect distribution used for the numerical calculations to get surface band bending.

In Fig.3 we tried to simulate results theoretically using D_{it} shown in Fig.2. From QSSPC measurements of the sample with a MOSOM structure, we obtained the effective lifetime τ_{eff} as a function of gate voltage V_g, which was converted to S_{eff} using Eq.1 (shown in the inset of Fig.3). The corresponding surface potential Ψ_s can be calculated through the extended SRH model[20] with an illumination level of Δn=1×10^{15}cm^{-3}, without consideration of charge in interfacial traps. From experimental data, $\Psi_{s,max}$ ~ -0.02V is found and induced σ_p/σ_n ~ 0.01, which is consistent with capture cross section of ALD Al_2O_3/c-Si interface measured by conductance method[21] and capture cross section of PECVD Al_2O_3/c-Si obtained by DLTS[22].

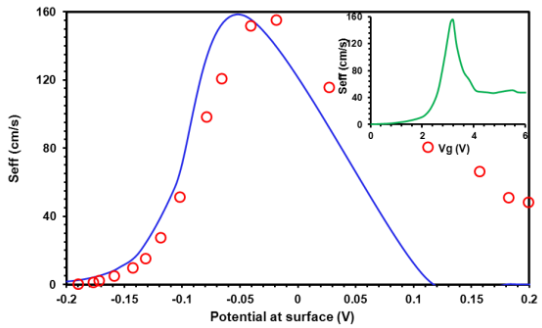

Fig.3 S_{eff} as a function of surface potential; Red open circles: experimental data. Blue curve: theoretically fitted curve based on the capture cross-section shown in Fig. 4 and extended SRH theory. Gate voltage dependence of effective surface recombination velocity obtained by QSSPC measurements are shown in the inset.

Then assumed capture cross section of electrons and holes as a function of trap energy(show in Fig.4) and measured D_{it} and Q_f (shown in Fig.2) were utilized to calculate theoretical relationship between surface potential and effective surface recombination velocity illustrated by the blue curve in Fig.3. During the simulation, σ_p / σn was adjusted to get similar $S_{eff\ max}$ as measured value. The shape of capture cross section distribution was assumed by reference of DLTS tested energy dependent capture cross section of PECVD Al_2O_3/c-Si interface[22]. We found that the simulated capture cross section for holes and electrons in this work is very similar to high-quality SiO_2/c-Si interface[23].

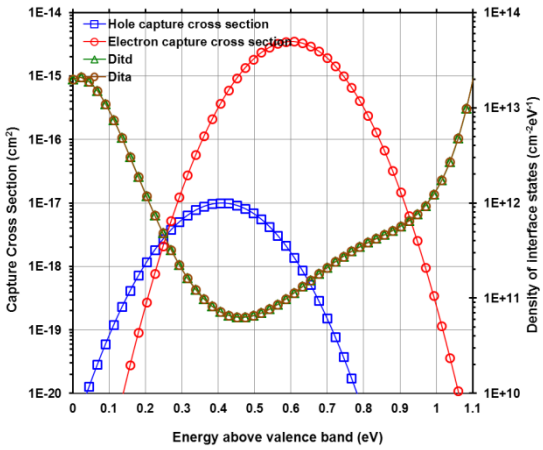

Fig.4. Simulated energy dependent capture cross sections for holes and electrons and energy dependent D_{it} obtained from capacitance-voltage measurement. It is assumed that acceptor type interface state density D_{ita} is equal to donor type interface state density D_{itd}.

We note that the capture cross section of electron is larger than that of hole, which is opposite to the assumption proposed in Part 1. The reason for the high effective surface recombination at inversion region will be investigated afterwards.

3. Field effect passivation by electron injection

CV samples were used to investigate the electron injection for Si/Al_2O_3 stack. Progressively increased positive or negative bias voltages were applied to the front metal contacts for periods of 60 seconds. Following each bias voltage, a high frequency C-V sweep was carried out from 0 volt to determine the flat band voltage V_{fb}.

In Fig.5(a), it can be clearly seen that V_{fb}, which is related to the fixed charge density in the Al_2O_3, shifts toward positive direction with increasing positive bias time and voltage. We note that higher voltage bias can continue shift the HF CV curve even though saturation has been observed for lower bias voltage cases. It is explained that positive bias results in more negative charge due to the injection of electrons into the aluminum oxide film, where they are trapped in Al_2O_3 , but the properties about the traps has not been investigated.[24]In this case, it is necessary to sweep from negative to positive to get reliable V_{fb} regardless of p-type or n-type substrates. It is interesting to find that negative bias can lead to electron injection as well, shown in Fig.5(b) and (d). We consider that only electron traps exist in PAALD Al2O3 layer and electrons from the negative biased electrode inject in Al2O3 layer in this case. We believe electron injection from silicon into Al_2O_3 could be used to enhance field effect passivation of Al_2O_3 as what has been applied on Si/SiN_x structures[25]. This could be used to improve the passivation performance of thin Al_2O_3, less than 10nm.

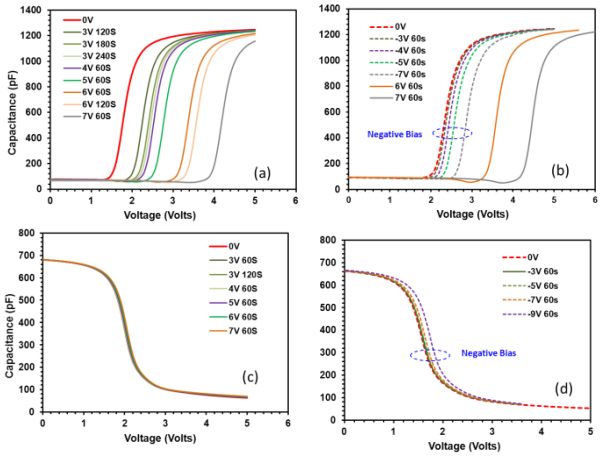

Fig5. High frequency CV curves with different positive bias voltage and bias time. (a) n-type wafer used for CV, deposition start at 150℃; (b) p-type wafers used for CV, deposition start at less than 150℃.

Fig. 5(c) illustrates that electron injection as a result of positive voltage bias is not always observed. Determination of the conditions that lead to the presence of chargeable defects is an area of current investigations. It is likely that the growth conditions during the first few cycles, such as deposition temperature and pre-deposition plasma generation time are very important to the electrical and physical properties of Al_2O_3, and also to the passivation performance.

It should be note that the difference of capacitance at accumulation for Fig. 5(a) and (c) is due to the size diversity of Al dot.

CONCLUSION

Field-effect passivation of plasma–assisted atomic layer deposition (PA-ALD) Al_2O_3 for p- and n- type c-Si was investigated by both positive corona charge and voltage-lifetime measurements. An unusual phenomenon of slight passivation performance recovery upon long time positive corona charge was observed, which is confirmed by another experiment applying gradual increasing positive voltage on a similar wafer. it was found that the maximum capture cross section of electrons is approximately 100 times larger than that of holes at the interface of Al_2O_3/c-Si. Field effect passivation related with fixed negative charge density can be improved by increased Al_2O_3 surface potential, such as positive voltage bias or corona charge and the ability of electron injection from silicon to Al_2O_3 can be controlled by changing Al_2O_3 deposition parameters.

REFERENCES

1. M. J. Kerr, A. Cuevas, Semiconductor science and technology 17, 35 (2002).
2. T. Lauinger, J. Schmidt, A. G. Aberle, R. Hezel, Applied Physics Letters 68, 1232 (Feb, 1996).
3. V. D. Mihailetchi, Y. Komatsu, L. Geerligs, Applied Physics Letters 92, 063510 (2008).
4. M. Taguchi et al., Progress in Photovoltaics: Research and Applications 8, 503 (2000).
5. S. Olibet, E. Vallat-Sauvain, C. Ballif, Physical Review B 76, 035326 (2007).
6. P. P. Altermatt et al., Journal of Applied Physics 92, 3187 (2002).
7. P. Altermatt et al., paper presented at the Proceedings of the 21st EU-PVSEC, Dresden, (2006).
8. D. Macdonald, L. Geerligs, Applied Physics Letters 85, 4061 (2004).
9. B. Hoex, J. Schmidt, P. Pohl, M. van de Sanden, W. Kessels, Journal of Applied Physics 104, 044903 (2008).
10. J. Benick et al., Applied Physics Letters 92, 253504 (2008).
11. B. Hoex et al., Applied Physics Letters 91, 112107 (2007).
12. K. Yasutake, Z. Chen, S. Pang, A. Rohatgi, Journal of Applied Physics 75, 2048 (1994).
13. W. Jellett, K. Weber, Applied Physics Letters 90, 042104 (2007).
14. S. Glunz, D. Biro, S. Rein, W. Warta, Journal of Applied Physics 86, 683 (1999).
15. A. B. Sproul, Journal of Applied Physics 76, 2851 (1994).
16. M. J. Kerr, A. Cuevas, Journal of Applied Physics 91, 2473 (2002).
17. W. Shockley, W. T. Read, Jr., Physical Review 87, 835 (1952).
18. R. N. Hall, Physical Review 87, 387 (1952).
19. R. Castagne, A. Vapaille, Surface Science 28, 157 (1971).
20. A. G. Aberle, S. Glunz, W. Warta, Journal of Applied Physics 71, 4422 (1992).
21. F. Werner, A. Cosceev, J. Schmidt, Journal of Applied Physics 111, 073710 (2012).
22. P. Saint-Cast et al., Energy Procedia 8, 642 (2011).
23. S. W. Glunz, Albert Ludwigs Universitat Freiburg Germany, Thesis (1991).
24. 24. J. J. H. Gielis, B. Hoex, M. C. M. v. d. Sanden, W. M. M. Kessels, Journal of Applied Physics 104, 073701 (2008).
25. Y. Ren, Trapping and Decay of Negative Charge in Silicon Nitride Films for Photovoltaic Applications, The Australian National University, Australia, Thesis (2011)